Nanoscale

Accepted Manuscript

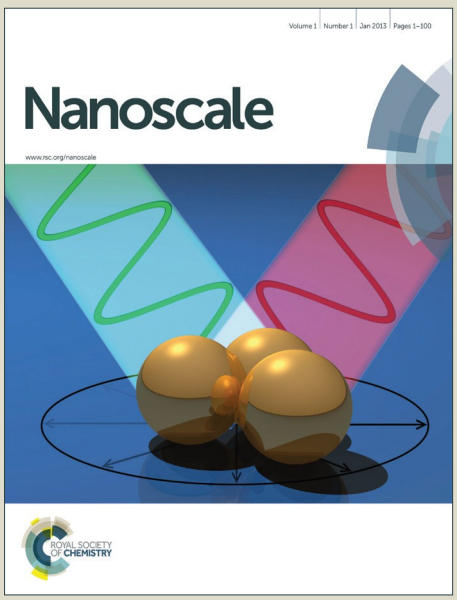

ROYAL SOCIETY OF CHEMISTRY

www.rsc.org/nanoscale

Fe_3O_4 MNPs and thermoplastic polyurethane (TPU) in an external magnetic field (Figure 1). Magnetometry measurements were conducted to evaluate the anisotropic magnetic properties of MPNC. Higher magnetization was obtained parallel rather than perpendicular to the MNP chains. Magnetic anisotropy associated by chaining MNPs is the prevailing kind of magnetic anisotropy in this system. The magnetization directions of the MNPs are determined by minimizing the magnetostatic energy, for which the dipolar interaction energy among the MNPs and the Zeeman energy generated by the applied field are the most significant terms. Assembly of the MNPs into chains causes a directional dependence in the magnetostatic energy, allowing for anisotropic actuation of the composite in 3D. Actuation experiments were conducted on a thin film composite sample cut into the shape of a cross, where the arms facilitate bending and the chains of MNPs point along two of the arms. The terms, "parallel arms" and "perpendicular arms" refer to orientations of the arms parallel and perpendicular to the chains, respectively. Actuation was investigated in both spatially uniform fields and field gradients.

In the spatially uniform, horizontal field of the electromagnet, the sample was supported in the center, while gravity caused the arms of the thin elastomer film to hang down, nearly vertically. Two orientations of the sample were studied (Figure 2a), parallel arms hanging to the left and right sides (LR) and parallel arms hanging to the front and back (FB). In orientation LR, as the field is increased, the parallel arms lift up toward horizontal, bringing the arms and MNP chains close to alignment with the field. The perpendicular arms are unaffected, since the chains are already aligned with the field. In orientation FB, the chains in all of the arms are oriented perpendicular to the field. Since the sample is pinned in the center, the field causes a twisting torque in each arm to bring the chains closer to alignment with the field. Rotating the sample within the gap of an electromagnet also shows a marked dependence on orientation. Periodicity in the lifting behavior of 360° was observed for the parallel arms (ESI†, Video S1 and Figure S2). At certain angles of rotation, the perpendicular arms snapped to obtain a new, more stable configuration. Snapping is caused by the release of elastic energy that accumulates as the arm twists.[41]

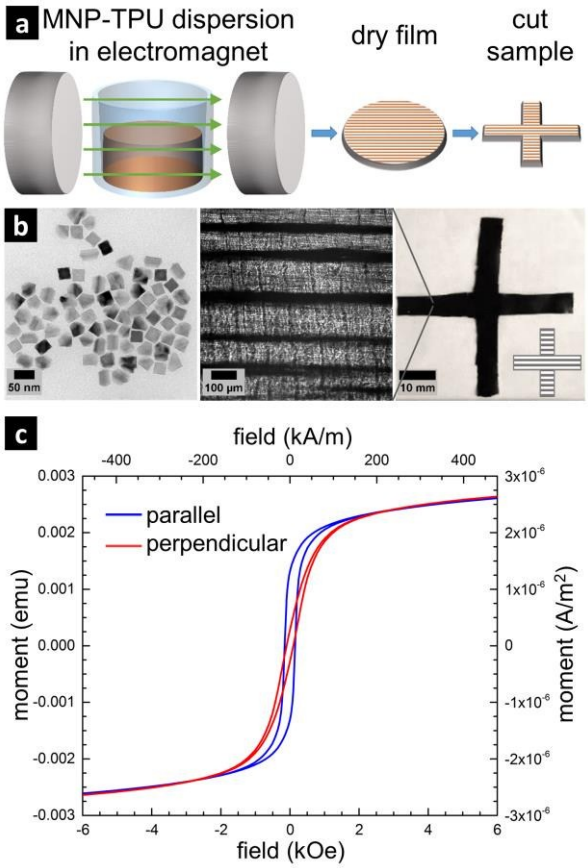

Figure 1. (a) Schematic for the process of preparing a chained magnetic polymer nanocomposite (MPNC) cross sample, (b) left to right: TEM image of magnetic nanoparticles (MNPs), optical micrograph of chained MPNC, photograph of cross sample, and (c) magnetometry of a chained MPNC at 300 K measured parallel and perpendicular to the chains.

For experiments in a magnetic field gradient, the sample was pinned in the center on a flat rotating stage, and a permanent magnet was held at a fixed height above the edge of the sample, such that the ends of the arms would pass beneath it (Figure 2b and ESI, Video S2). Only the parallel arms lift toward the magnet as they are rotated below. If the MNPs had been dispersed uniformly in the elastomer without chaining, the same result would be expected for all four arms, either lifting if the magnetic force overcomes gravity, or not lifting if gravity prevails. Selective lifting of the parallel arms can be understood from the magnetic force (Figure 2c), which is the negative gradient of the magnetostatic energy. The magnetic force is strongest when the moments point in the direction of the field gradient. For both perpendicular and parallel configurations, the field causes (via the Zeeman energy) magnetic moments of the MNPs to tilt toward the field direction, and the field gradient generates an attractive lifting force toward the permanent magnet. The magnetization of the chained MNPs in the direction of the field gradient is expected to be higher for the parallel arms than for the perpendicular arms, which is consistent with the higher magnetization of parallel than perpendicular chains at a given field, observed in magnetometry measurements (Figure 1c). Furthermore, magnetizing the parallel arm causes increasingly favorable dipolar coupling as the arm lifts up, generating a sufficient force to overcome gravity. Dipolar coupling in the perpendicular arm under the permanent magnet reduces the magnetization in the direction of the field gradient; the resulting force is too weak to lift the perpendicular arm. As the sample rotates, aligning the field lines with the perpendicular arms is expected to generate twisting rather than lifting, which is observed as a minor deflection in their ends as they pass beneath the permanent magnet. The selectivity of lifting depends on the distance between the sample and the magnet. At significantly shorter separations, both parallel and perpendicular arms lift, while neither arm lifts at longer distances.

It is also important to consider potential non-magnetic effects caused by assembling the MNPs on the bending modulus of the composite, for example due to particle jamming. Mechanical deformation tests on chained MPNCs have sho

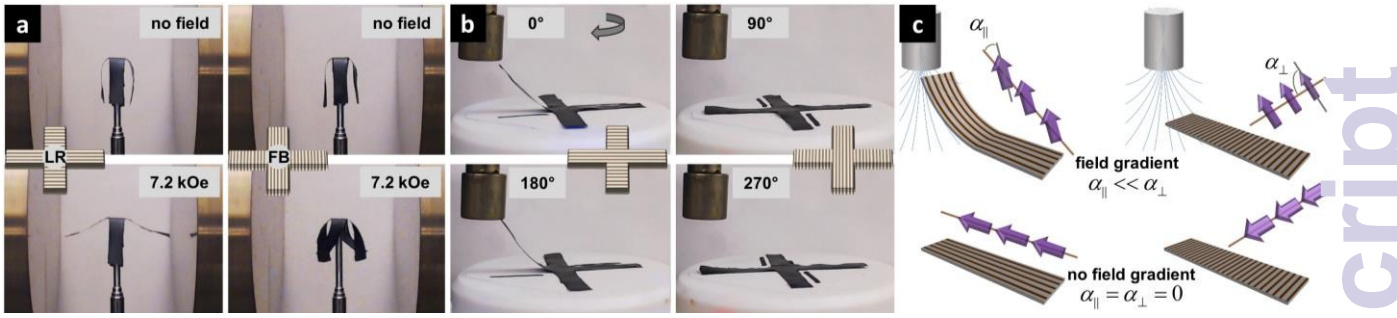

Figure 2. Photos showing anisotropic actuation under (a) uniform magnetic field (7.2 kOe, 570 kA/m) for the cross mounted by its center, where the chains for th flattened cross would be aligned (left) parallel (LR) to the field and (right) perpendicular (FB) to the field, and (b) field gradients from a permanent magnet that selective lifts parallel but not perpendicular arms as the sample is rotated. (c) schematic showing relative orientation of MNP dipoles with respect to the chain direction in th presence and absence of field lines generated by a permanent magnet, which causes selective lifting in (b). See ESI, Videos S1-2 for movies of these lifting processes.

that MNP chains increase the modulus parallel to them.[42,43] Therefore, the modulus for bending the parallel arms is expected to be higher than for the perpendicular arms, if the MNPs would have a structural effect. Selective lifting of the parallel arms despite the potential increase in modulus caused by chaining indicates that the magnetic, rather than structural, anisotropy of the MPNC is the dominant effect in these experiments.

To better understand the actuation mechanism, the bending angle of the parallel arms aligned with the field of an electromagnet (orientation LR in Figure 2a) was measured as a function of the horizontal magnetic field strength, H. As H increases, the arms lift higher toward horizontal, decreasing the bending angle, θ. A simple model (see ESI for details) was constructed for interpreting this experiment. The equilibrium positions of the arm and of the magnetic moments within the arm are obtained by balancing the mechanical torques on the arm and the magnetic torques on the MNP moments. Linear, continuous chains of touching spherical MNPs with negligible interchain interactions are used to model the MPNC. Two

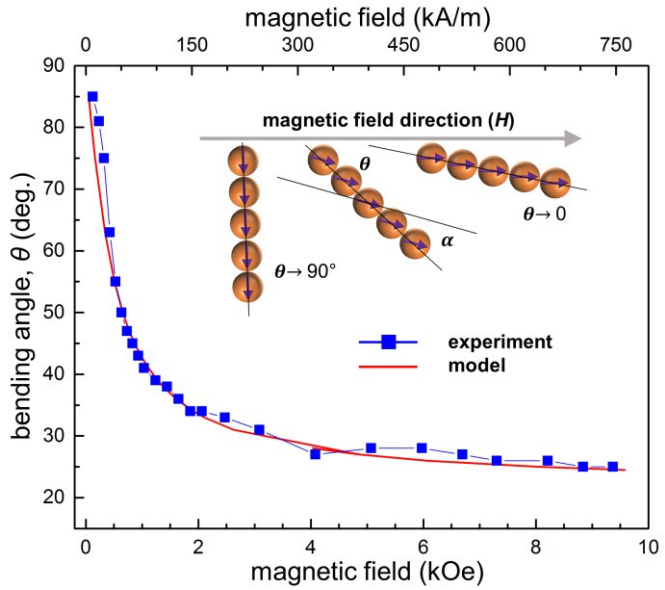

Figure 3. Plots of the bending angle θ, as a function of the applied uniform magnetic field for experimental data and the model.

magnetic forces generate torques on the moments: dipola interactions between MNPs, which favor alignment with th chain direction, and the Zeeman energy, which favors alignmen with the direction of the applied field. The model of the torq on the moments mimics the Stoner-Wohlfarth model for the magnetization of single-domain, single-crystal magn particles, where the Zeeman energy is balanced by crystal anisotropy.[44] Two forces generate mechanical torques on arm: gravity and dipolar interactions between MNPs, whic favors alignment of the arm with the moments in the chains thereby generating more favorable head-to-tail interactio and fewer side-by-side interactions. Dipolar interactio between MNPs therefore affect equilibrium of both the moments and the arm. The process of lifting the arm up towar the field direction can be understood as follows: The applied magnetic field rotates the moments slightly out of the chai direction (at a "moment angle," α) and toward the applied field direction, causing less favorable dipolar interactions among th moments. Lifting the arm toward the field direction gives more favorable dipolar interactions while also allowing the momen to point toward the field direction and reducing α.

In the experimental sample, the chains are multiple MN wide (Figure 1b), as also noted elsewhere.[19,32] The chain width has not been accounted for in this model of chains of a single MNP in width. A disorder parameter (γ) is introduced to accoun for the accompanying magnetic disorder within the chains. I disordered chains, saturation of the moments along the ch axis causes side-by-side interactions along with favorable head to-tail interactions. We compensate for the side-by-sid interactions by multiplying the moment of the MNP by γ, wher $0 \le \gamma \le 1$. The limit $\gamma = 1$ corresponds to the perfect chain described by the model without correction, and $\gamma = 0$ would describe an isotropic arrangement of moments without chaining direction. The value of γ has been approximated as th remanent magnetization divided by the saturatio magnetization (M_R/M_S) for measurements parallel to the chain direction. This is a reasonable approximation,[45] because perfect chain would theoretically have $M_R = M_S$.

According to the model, at equilibrium

$$H = 0.598 \frac{\cos\theta}{\sin(\theta - \alpha)} \text{ kOe, where } \sin 2\alpha = 0.742\cos\theta .$$ When

this expression for θ vs. H is plotted along with the experimental data, γ = 0.445 from magnetometry gives an excellent match (Figure 3), which is remarkable for a simple model with a single, experimentally determined parameter. The maximum value of α is less than 0.4° (ESI, Figure S2), which suggests the moments remain nearly aligned with the chain direction. Several simplifying assumptions, described in the ESI, have been made about the magnetic properties of the MNPs. It should further be noted that the mechanical properties of the polymer have been neglected in this model; the mechanical response of the MPNC is determined solely by the magnetic behavior of the chains rather than the mechanical properties of the polymer. The good agreement between the model and the experimental system, however, indicates that the properties of such anisotropically responsive materials can be predicted and controlled by corresponding adjustments in the magnetic characteristics of the MNPs and their arrangement within the polymer.

Conclusions

In conclusion, we have demonstrated and modeled the anisotropic response of a chained MPNC via selective and directional bending of the arms of a large elastomer film. The interaction of the magnetic anisotropy of the chains with magnetic fields and field gradients allows for controlled actuation of these macroscale samples in 3D. These flexible thin films with magnetically driven, directional mechanical responses can be employed for remote directional manipulation of soft actuators, valves, motors, and other soft robotics applications.

Acknowledgements

This research was supported by the National Science Foundation (DMR-1056653 and the Research Triangle MRSEC, DMR-1121107). Huntsman Corporation is acknowledged for providing the elastomer used in this study. The authors also acknowledge Peter Krommenhoek for training in nanoparticle synthesis and use of the electromagnet, Lewis Reynolds for assistance with magnetometry measurements, Catherine Marcoux and Joshua Socolar for advice about modeling, and the use of the Analytical Instrumentation Facility (AIF) at North Carolina State University, which is supported by the State of North Carolina and the National Science Foundation.

References

1 M. Zrínyi, L. Barsi and A. Büki, *J. Chem. Phys.*, 1996, **104**, 8750–8756.
2 M. Khoo and C. Liu, *Sens. Actuators A*, 2001, **89**, 259–266.
3 J. J. Mack, B. N. Cox, M. Lee, J. C. Y. Dunn and B. W. Wu, *J. Mater. Sci.*, 2007, **42**, 6139–6147.
4 P. Garstecki, P. Tierno, D. B. Weibel, F. Sagués and G. M. Whitesides, *J. Phys. Condens.: Matter*, 2009, **21**, 204110.
5 S. Ghosh and T. Cai, *J. Phys. D: Appl. Phys.*, 2010, **43**, 415504.
6 M. Yoonessi, J. A. Peck, J. L. Bail, R. B. Rogers, B. A. Lerch and M. A. Meador, *ACS Appl. Mater. Interfaces*, 2011, **3**, 2686–2693.
7 K. Zimmermann, V. A. Naletova, I. Zeidis, V. A. Turkov, E. Kolev, M. V. Lukashevich and G. V. Stepanov, *J. Magn. Magn. Mater.*, 2007, **311**, 450–453.
8 B. A. Evans, A. R. Shields, R. L. Carroll, S. Washburn, M. R. Falvo and R. Superfine, *Nano Lett.*, 2007, **7**, 1428–1434.
9 L. Zhang, J. J. Abbott, L. Dong, B. E. Kratochvil, D. Bell and B. J. Nelson, *Appl. Phys. Lett.*, 2009, **94**, 064107.
10 M. S. Sakar, E. B. Steager, D. H. Kim, M. J. Kim, G. J. Pappas and V. Kumar, *Appl. Phys. Lett.*, 2010, **96**, 043705.
11 N. Inomata, T. Mizunuma, Y. Yamanishi and F. Arai, *J. Microelectromech. Syst.*, 2011, **20**, 383–388.
12 J. J. Benkoski, R. M. Deacon, H. B. Land, L. M. Baird, J. L. Breidenich, R. Srinivasan, G. V. Clatterbaugh, P. Y. Keng and J. Pyun, *Soft Matter*, 2010, **6**, 602–609.
13 A. C. Balazs, T. Emrick and T. P. Russell, *Science*, 2006, **314**, 1107–1110.
14 C. F. Hayes, *J. Colloid Interface Sci.*, 1975, **52**, 239–243.
15 R. W. Chantrell, A. Bradbury, J. Popplewell and S. W. Charles, *J. Appl. Phys.*, 1982, **53**, 2742–2744.
16 J. E. Martin, E. Venturini, J. Odinek and R. A. Anderson, *Phys. Rev. E: Stat. Nonlinear Soft Matter Phys.*, 2000, **61**, 2818–283
17 Y. Sahoo, M. Cheon, S. Wang, H. Luo, E. P. Furlani and P. N. Prasad, *J. Phys. Chem. B*, 2004, **108**, 3380–3383.
18 V. S. Abraham, S. S. Nair, S. Rajesh, U. S. Sajeev and M. R. Anantharaman, *Bull. Mater. Sci.*, 2004, **27**, 155–161.
19 W.-X. Fang, Z.-H. He, X.-Q. Xu, Z.-Q. Mao and H. Shen, *Europhys Lett.*, 2007, **77**, 68004.
20 R. M. Erb, R. Libanori, N. Rothfuchs and A. R. Studart, *Science*, 2012, **335**, 199–204.
21 Q. Zhang, M. Janner, L. He, M. Wang, Y. Hu, Y. Lu and Y. Yin, *Nano Lett.*, 2013, **13**, 1770–1775.
22 K. Butter, P. H. H. Bomans, P. M. Frederik, G. J. Vroege and A. P Philipse, *Nat. Mater.*, 2003, **2**, 88–91.
23 E. Alphandéry, Y. Ding, A. T. Ngo, Z. L. Wang, L. F. Wu and M. P. Pileni, *ACS Nano*, 2009, **3**, 1539–1547.
24 S. Mørup, M. F. Hansen and C. Frandsen, *Beilstein J. Nanotechnol.*, 2010, **1**, 182–190.
25 J. B. Tracy and T. M. Crawford, *MRS Bull.*, 2013, **38**, 915–920.
26 B. Bharti, A.-L. Fameau, M. Rubinstein and O. Velev, *Nat. Mater.*, in press.
27 N. A. Yusuf, *J. Phys. D: Appl. Phys.*, 1989, **22**, 1916.
28 C.-Y. Hong, *J. Appl. Phys.*, 1999, **85**, 5962–5964.
29 D. Lorenzo, D. Fragouli, G. Bertoni, C. Innocenti, G. C. Anyfantis, P. D. Cozzoli, R. Cingolani and A. Athanassiou, *J. Appl. Phys.*, 2012, **112**, 083927.
30 S. L. Saville, R. C. Woodward, M. J. House, A. Tokarev, J. Hammers, B. Qi, J. Shaw, M. Saunders, R. R. Varsani, T. G. S. Pierre and O. T. Mefford, *Nanoscale*, 2013, **5**, 2152–2163.
31 J. W. Swan, J. L. Bauer, Y. Liu and E. M. Furst, *Soft Matter*, 2014, **10**, 1102–1109.
32 P. J. Krommenhoek and J. B. Tracy, *Part. Part. Syst. Charact.*, 2013, **30**, 759–763.
33 Y. Yao, E. Metwalli, M. A. Niedermeier, M. Opel, C. Lin, J. Ning, J. Perlich, S. V. Roth and P. Müller-Buschbaum, *ACS Appl. Mater. Interfaces*, 2014, **6**, 5244–5254.
34 J. Kim, S. E. Chung, S.-E. Choi, H. Lee, J. Kim and S. Kwon, *Nat. Mater.*, 2011, **10**, 747–752.
35 T.-R. Ger, H.-T. Huang, W.-Y. Chen and M.-F. Lai, *Lab. Chip*, 2013 **13**, 2364.
36 J. A. Kim, S. H. Lee, H. Park, J. H. Kim and T. H. Park, *Nanotechnology*, 2010, **21**, 165102.

37 D. Yang, W. Huang, X. He and M. Xie, *Polym. Int.*, 2012, **61**, 38–42.
38 J. A. Medford, J. W. Hubbard, F. Orange, M. J.-F. Guinel, B. O. Calcagno and C. Rinaldi, *Colloid Polym. Sci.*, 2014, **292**, 1429–1437.
39 J.-C. Kuo, H.-W. Huang, S.-W. Tung and Y.-J. Yang, *Sens. Actuators A*, 2014, **211**, 121–130.
40 F. Lu, A. Popa, S. Zhou, J.-J. Zhu and A. C. S. Samia, *Chem. Commun.*, 2013, **49**, 11436.
41 N. P. Bende, A. A. Evans, S. Innes-Gold, L. A. Marin, I. Cohen, R. C. Hayward and C. D. Santangelo, *arXiv:1410.7038 [cond-Mat.soft]*, 2014.
42 M. R. Jolly, J. D. Carlson, B. C. Muñoz and T. A. Bullions, *J. Intell. Mater. Syst. Struct.*, 1996, **7**, 613–622.
43 Z. Varga, G. Filipcsei and M. Zrínyi, *Polymer*, 2005, **46**, 7779–7787.
44 E. C. Stoner and E. P. Wohlfarth, *Philos. Trans. R. Soc. A*, 1948, **240**, 599–642.
45 S. Kan, M. Sachan, J. Kirchhoff and S. A. Majetich, *IEEE Trans. Magn.*, 2005, **41**, 3370–3372.

Table of Contents Entry

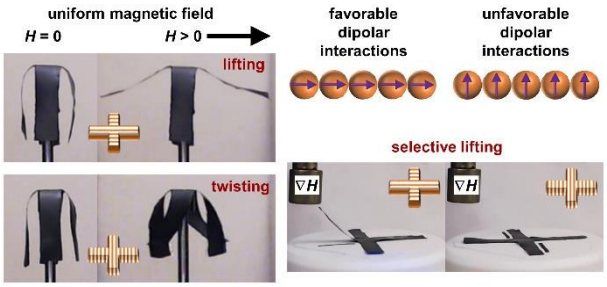

One-dimensional arrangement of magnetic nanoparticles in chains imparts anisotropy to their magnetic response, which is used for mechanical 3D actuation.